

pubs.acs.org/acscatalysis Research Article

Stereoblock vs Stereoblend: Orchestrating Competing Living Coordination Chain Transfer Polymerizations for the One-Pot Production of New Viscoelastic Grades of Poly(4-methyl-1-pentene)

Danyon M. Fischbach, Charlotte M. Wentz, Saeid Mehdiabadi, João Soares, and Lawrence R. Sita*



Cite This: ACS Catal. 2024, 14, 2333-2340



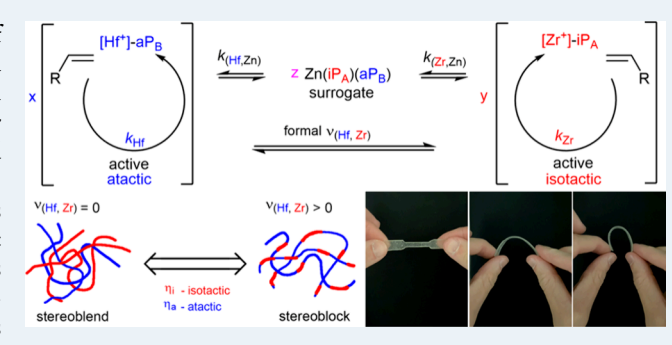
ACCESS

Metrics & More

Article Recommendations

Supporting Information

ABSTRACT: By exerting control over two populations of coexisting cyclopentadienyl, amidinate (CPAM) group 4 metal active species that possess different stereoselectivities for chain growth propagation during the living coordinative chain transfer polymerization (LCCTP) of 4-methyl-1-pentene, controlled production of grades for poly(4-methyl-1-pentene) (PMP) materials that display a tunable range of viscoelastic properties can be achieved in "one-pot" fashion. Analytical and spectroscopic investigations reveal that these differences in viscoelastic properties are associated with formation of atactic/isotactic PMP stereoblends, rather than a stereoblock chain architecture. These results serve to establish the ability of low molar mass atactic PMP to



function as an effective property modifier for commercially important isotactic PMP, which in its pure form is highly brittle with low tensile strength. The further outcome of these studies is extension of multistate LCCTP as a tool for expanding the range of accessible grades and properties of polyolefins that can be produced from the limited small set of industrially significant olefins.

KEYWORDS: tacticity, living, chain transfer, polymerization, polyolefin

Polyolefins will continue to be critical for supporting technological advancement of humanity for the foreseeable future. This position of importance is guaranteed by the longterm sustainability of abundant and inexpensive olefin feedstock monomers that can be easily converted on an enormous industrial scale into a vast range of different classes and grades of polyolefin materials that possess a broad spectrum of physical properties required for different applications, such as ethene (C2) and propene (C3) for production of polyethene (PE)- and polypropene (PP)-based materials, respectively.1 On the other hand, the staggering global volume of plastic waste from all commercial polymers that is accumulating in the environment, of which polyolefins now comprise 50%, is an enormous challenge facing society that must be solved in the near and long term. In this regard, a holistic approach not only involves the design and implementation of new strategies for increasing levels of collection, recycle, and repurposing of plastic waste, but also an increase in the production and utilization of "green" commercial polymers that have an overall negative carbon footprint and that do not degrade into chemical byproducts that have an adverse environmental impact. 3,4 Perhaps counterintuitively, polyolefins fit this profile as they can be produced from biosourced "green" olefin feedstocks that have very high CO2 capture quotients, as exemplified by Braskem's new grades of green PE, and as pure hydrocarbons, they are

biologically benign. New advances are also being made with the development of chemical processes that can convert polyolefin waste into useful chemicals and lower molar mass materials with an increased net energy savings. 5 Accordingly, there are significant long-term advantages and rewards for identifying and developing new classes of green polyolefins, of which poly(4-methyl-1-pentene) (PMP) can be classified as one since the requisite 4-methyl-1-pentene (4M1P) monomer is currently produced on a large industrial scale through the alkali-metal catalyzed dimerization of C3, which is increasingly being biosourced. Highly stereoregular isotactic PMP (iPMP) is a commercial thermoplastic polyolefin with a high melting temperature, $T_{\rm m}$, of 250 °C, excellent optical transparency, and a low dielectric constant that is useful for a range of applications, including microwave cookware, optical lenses, and acoustic coverings, to name a few. However, a critical disadvantage of iPMP is that molded films are highly brittle with a low impact and tensile strength. Herein, we present the

Received: November 17, 2023 Revised: January 10, 2024 Accepted: January 10, 2024 Published: January 30, 2024

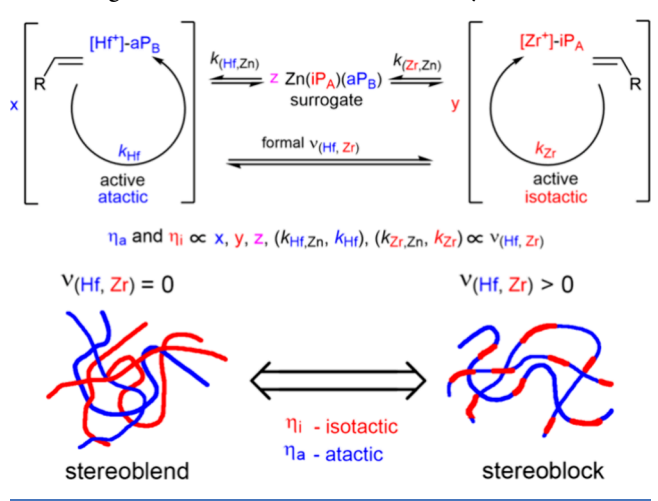




results of a successful project undertaken to develop new viscoelastic grades of PMP through extension of "multistate" living coordinative polymerization (LCP) and living coordinative chain transfer polymerization (LCCTP) as a toolbox of processes for greatly expanding the range of new forms and properties of polyolefins that can be produced from the very small set of industrially relevant commodity olefin feed-stocks. $^{\rm 2b,8-10}$

Scheme 1 presents the new multistate strategy that is the subject of the present report in which isospecific and aspecific

Scheme 1. Two-State Competing LCCTP Strategy for Producing New Viscoelastic Grades of Polyolefins

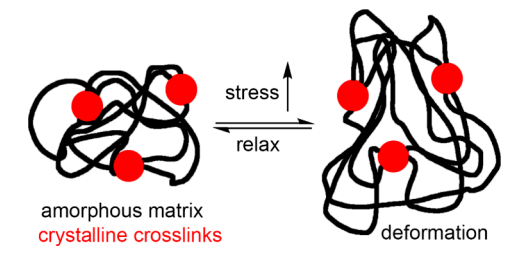


LCCTP processes for 4M1P are pitted against each other within a single reactor using varying equivalents of diethylzinc, ZnEt₂ (DEZ), as a chain transfer agent (CTA). As with other multistate LCP and LCCTP processes that we have proposed and experimentally validated, in the absence of chain termination, all the desired features of a living polymerization can be retained if the rate and rate constants for reversible group and polymeryl chain transfer between active transitionmetal propagators and either dormant species, in the case of LCP, or an excess population of main-group-metal "surrogate" chain growth centers, in the case of LCCTP, are far greater in magnitude than the corresponding kinetic parameters for chain growth occurring at the transition-metal centers. 9,10 This includes the ability to have control over the number-average degree of polymerization, DPn, and a very narrow molar mass distribution (MMD), as defined by a dispersity index, D (= $M_{\rm w}/M_{\rm n} \leq 1.1$, where $M_{\rm n}$ and $M_{\rm w}$ are the number-average and weight-average molar mass indices. However, the key advantage of multistate LCP and LCCTP processes lies with introduction of new mechanistic control points that can be manipulated and brought under external control to direct product formation as an infinite variety of different grades with differing properties that formally exist within a spectrum defined by two limiting ends. Recently, we have successfully employed two-state stereomodulated LCP to produce new fundamental grades of amorphous, atactic PMP (aPMP) and a series of semicrystalline iPMP materials possessing various levels of stereoerror incorporation. We have also previously employed temporal control over this two-state stereomodulated LCP process to produce a family of stereoblock polypropene (sbPP) thermoplastic elastomers that are composed of atactic and isotactic block domains of discrete

number-average length, η_a and η_{iv} respectively, and that are strung together in programmed fashion (e.g., atactic-isotactic diblock vs isotactic-atactic-isotactic triblock).8,11 We have further designed and validated multistate LCCTP processes in which kinetic parameters associated with two different CTAs can be controlled to manipulate MMD within a family of polyolefin grades, and in which the ratio of two different coinitiators for activating a single preinitiator can be used to control copolymer composition by manipulating relative reactivity ratios of the two monomers in a predictable fashion under otherwise identical reactor conditions. 9c,d In another take on multistate LCCTP, we have also recently shown that the optical purity of a chiral preinitiator, as established by premixing the two pure enantiomers in different ratios, can be used to control stereoregularity (tacticity) within a targeted family of polyolefin grades. 9h Finally, by effecting temporal control over multistate LCCTP, we have also shown that no limits exist for producing an infinite number of new grades of a polyolefin from a single olefin monomer with respect to the ability to program different variations in the width and modality (e.g., mono-, bi-, and multimodal) of the MMD profile.9

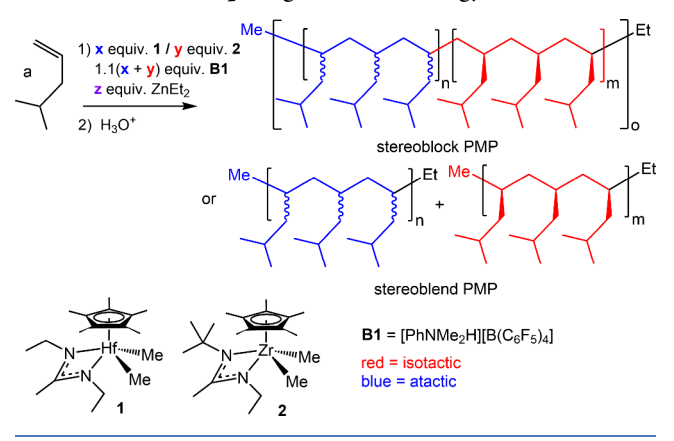
Returning back to the multistate mechanism of Scheme 1, the rate of chain transfer, $\nu_{(Hf,Z_r)}$, that can formally occur between the aspecific Hf propagator, which is known to produce an atactic polyolefin microstructure, and the stereospecific Zr active species, which propagates in isotactic fashion, is dependent upon a number of kinetic variables, including the relative population size of all the active and surrogate chain growth centers, as established by the initial stoichiometric equivalents for x, y, and z (see Scheme 1), as well as the rate constants for propagation at each of the two transition-metal active centers (cf. k_{Hf} and k_{Zr}) relative to those for reversible chain transfer occurring between each of the transition-metal propagators and the excess number of CTA-derived surrogates (cf. $k_{\text{(Hf, Zn)}}$ and $k_{\text{(Zr, Zn)}}$). More simplistically, as presented in Scheme 1, it can be seen that the possible range of values of η_a and η_i , which are a function of $\nu_{(Hf,Z_r)}$, comprise a spectrum of different stereochemical grades that is represented by a limiting isotactic-atactic stereoblend composition at one end, in the case of $\nu_{(Hf,Zr)}$ = 0, and uniform stereoblock microstructures for all other cases in which $\nu_{(Hf,Zr)} > 0$. It is also reasonable to conclude that the molar mass indices and MMD profile for each grade produced will further depend upon the relative rates and rate constants of all the inter- and intramolecular dynamic processes that are involved. 11 With respect to the goal of producing new viscoelastic grades of PMP, there is ample precedent in the literature for PP to show that this can likely be achieved by producing either isotactic-atactic stereoblends or "blocky" chain architectures so long as crystalline, isotactic-rich domains can serve as physical cross-links within an amorphous matrix composed of either atactic chains, or the noncrystallized portions of isotactic chains according to Scheme 2. 12,13 As a first-order approximation, the number and size of these crystalline cross-links relative to the amorphous matrix will determine bulk viscoelastic properties, irrespective of the materials being stereoblend or stereoblock in nature. Finally, the advantage of producing the former in a one-pot process is that it avoids any potential post polymerization degradation of molar mass and MMD that might occur with mechanical blending or the increase in chemical waste that is incurred with solvent blending of the different components.

Scheme 2. Origin of Differences in Viscoelastic Properties of Different Grades of Stereoblends and Blocky Stereoblock Polyolefins



Scheme 3 presents the experimental methods that were employed to investigate the viability of Scheme 1 for delivering

Scheme 3. Experimental Methods Employed to Investigate the Two-State Competing LCCTP Strategy of Scheme 1



new viscoelastic grades of PMP and Table 1 provides results obtained from these efforts. To begin, as we have previously reported, 10 run 0 serves as a benchmark for production of amorphous aPMP (Ia) using only the C_s -symmetric cyclopentadienyl, amidinate (CPAM) hafnium dimethyl preinitiator 1 in combination with 1.1 equiv of the anilinium borate, $[PhNHMe_2][B(C_6F_5)_4]$ (B1), as co-initiator and 5 equiv of DEZ as CTA. 8,9,14 Runs 1–9 document results obtained with an increasing amount of the chiral (but racemic) C_1 -symmetric CPAM zirconium dimethyl preinitiator 2 being introduced

while keeping the total number of transition-metal active propagators (Hf + Zr) and the number of equivalents of CTA constant. Finally, run 10 serves to provide the other benchmark in which use of only 2 as the preinitiator, and with all other factors remaining the same, produced highly crystalline iPMP (Ib).

Intriguingly, the PMP materials from runs 0–10 physically display striking differences in bulk viscoelastic properties that are also captured in the stress–strain curves obtained from dynamic mechanical analysis (DMA) using molded rectangular test samples, some of which are reproduced in Figure 1. Most

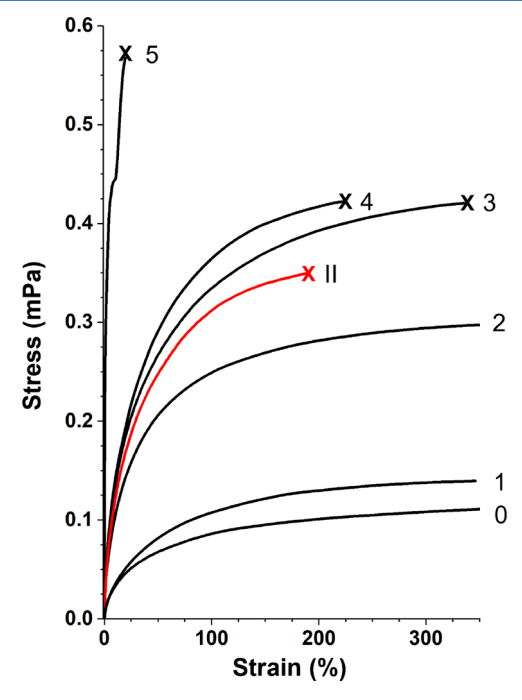


Figure 1. Stress—strain curves from DMA of selected samples from Table 1 (black) and actual blend of aPMP and iPMP (II) (red). Numerals refer to run numbers, and X signifies a breaking point.

notably, whereas the **Ia** sample (run 0) is amorphous with low tensile strength, there is a clear increase in the Young's modulus of the PMP samples with an increase in the amount of preinitiator **2** that was employed for their production (*cf.*,

Table 1. Poly(4-methyl-1-pentene) (I) Obtained by Two-State Competing LCCTP According to Scheme 3^a

run	1:2	yield (g)	$\frac{\mathbf{Ia} \ M_{\rm n}}{(\mathrm{kDa})^c}$	Ia D^c	$\begin{array}{c} \textbf{Ib} \ M_{\rm n} \\ {\rm (kDa)}^c \end{array}$	Ib Đ ^c	$({}^{\circ}C)^{d}$	$(^{\circ}C)^{d}$	crystallinity (%) ^d	Young's modulus (MPa) ^e	elongation at break (%) ^e
0	100:0	1.98	1.6	1.15			23			0.77	350
1	90:10	1.97	1.3	1.19	20.2	1.47	13	196, 208	0.92	1.04	346
2	80:20	1.78	1.4	1.20	39.0	1.40	7	203, 212	1.92	1.25	346
3	70:30	1.88	1.7	1.20	39.4	1.70	20	209, 217	4.70	3.01	336
4	60:40	1.67	1.6	1.16	40.6	1.65	18	215, 221	5.12	3.97	225
5	50:50	1.89	1.0	1.36	28.0	2.12	19	216, 222	10.9	38.8	19.4
6	40:60	1.86	0.9	1.18	37.3	2.14	13	215, 220	13.0	nd	nd
7	30:70	1.99	0.8	1.12	33.0	1.50		217	18.1	nd	nd
8	20:80	1.89	0.5	1.27	24.9	3.00		220	23.3	nd	nd
9	10:90	1.73	2.8	2.00	27.0	1.40		221	25.7	nd	nd
10	0:100	1.46			1.8	3.65		209	17.2	nd	nd
11	0:100 ^b	1.91			36.7	1.90		227	29.9	nd	nd

^aFor details of polymerization conditions for each run, see the SI. ^bNo chain transfer agent in run 11. ^cDetermined by SEC. ^dDetermined by DSC. ^eDetermined by DMA.

runs 1-5 in Figure 1), and then the sample becomes very brittle at the limit for the **Ib** sample (run 10) as expected. The photographic evidence of Figure 2 further shows the striking



Figure 2. Photos of PMP from run 3 (top) and iPMP from run 10 (bottom) subjected to a deformable strain.

difference in the elastic properties of PMP from run 3 that allows molded objects to be easily and reversibly deformed versus the very brittle nature of **Ia** from run 10.

Data obtained from ¹³C{¹H} NMR and differential scanning calorimetry (DSC) characterization of the complete set of new PMP grades of Table 1, as presented in Figure 3 and the

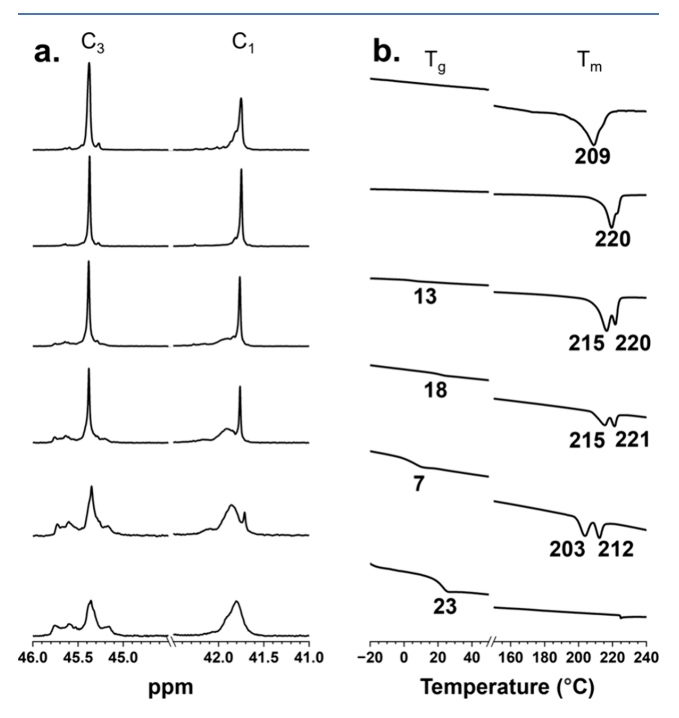


Figure 3. (a) Partial $^{13}\text{C}\{^1\text{H}\}$ (200 MHz, TCE- d_2 , 110 °C) NMR spectra showing ^{13}C resonances for C_1 and C_3 of PMP and (b) partial DSC traces of the second heating ramp (10 °C/min), with bold numbers indicating measured $T_{\rm g}$ and $T_{\rm m}$ values, obtained for runs 0, 2, 4, 6, 8, and 10 of Table 1 (bottom to top).

Supporting Information, appeared to support the preliminary conclusion that the observed differences in viscoelastic properties can be attributed to formation of an isotactic—atactic stereoblock architecture. More to the point, the collection of partial $^{13}C\{^{1}H\}$ (200 MHz, 1,1,2,2-tetrachloroethane-d₂ (TCE- d_2), 100 °C) spectra presented in Figure 3a for a subset of these materials (runs 0, 2, 4, 6, 8 and 10) show the expected broad ^{13}C resonances for C1 and C3 of Ia (run

0), whereas those for **Ib** (run10) are much narrower (sharper). Importantly, as previously reported, Ib produced under LCCTP conditions with preinitiator 2 contains a certain level of mmrm stereoerrors, where m and r designate meso and rac dyad configurations, 15 as the result of zinc-mediated chain exchange occurring between the two configurationally stable enantioforms of the zirconium-based active propagators. 9e,16 In between these two limiting reference samples, the ¹³C{¹H} NMR spectra show a superposition of ¹³C resonances for aPMP and iPMP, with the former diminishing in intensity relative to the latter as the run number increases (cf, runs 2, 4, 6, and 8). The trends observed in the NMR spectra are mirrored in the DSC data for these PMP materials, as presented in Figure 3b. For example, amorphous Ia reveals only a glass transition temperature while semicrystalline Ib displays a $T_{\rm m}$ of 209 °C, which is lower than that of commercial iPMP due to molar mass differences in M_n and Dand the aforementioned level of mmrm stereoerrors. As the proportion of iPMP increases relative to aPMP, there is an onset of crystallinity and an increase in $T_{\rm m}$ and crystallinity values through the progression of runs according to Table 1 and Figure 3b. Oddly though, the T_m value of 220 °C observed for PMP produced with a preinitiator ratio of 1: 2 set at 20:80 (run 8) is significantly higher than the iPMP reference Ib (run 10). This suggests that the iPMP content of the former material might be more stereoregular than that of the latter, even though both were presumably produced under reversible CT conditions. In support of this hypothesis, run 11 of Table 1 presents results for production of highly stereoregular iPMP that is devoid of any r dyads by using preinitiator 2 in the

absence of any CTA to yield a $T_{\rm m}$ value of 227 °C. Ever since Natta 12b first proposed an isotactic—atactic stereoblock architecture to rationalize the elastic properties of an isolated fraction of PP from a complex mixture of different tacticities, there has been considerable interest in developing new polymerization processes that could be used to produce stereoblock polyolefins on demand and with control over the viscoelastic properties of different grades of these materials through programmed variations in η_a and η_i . While we have previously been successful in achieving this goal for production of well-defined isotactic-atactic stereoblock PP thermoplastic elastomers through development of stereomodulated LCP based on temporal control over degenerate exchange between populations of configurationally stable (active) and configurationally unstable (dormant) states, this strategy suffers from the inability to scale the process to provide substantial amounts of product.8c Hence the strong desire to develop an LCCTP process based on enantiomerically pure and configurationally stable propagators. However, the historical record covering the quest for stereoblock polyolefins produced under chain transfer conditions is wrought with questions regarding the true nature of the materials actually produced. 17 Accordingly, even though all signs revealed so far pointed to the successful production of stereoblock PMP, we sought to avoid making a mistake. Thus, to begin, Soxhlet extraction of the PMP sample from run 5 was performed using refluxing hexanes for 18 h to provide 59% by weight of a soluble fraction with the remainder being insoluble.¹⁴ As presented in Figure 4, characterization by ¹³C{¹H} NMR and DSC unequivocally revealed these soluble and insoluble fractions to be aPMP and iPMP, respectively. Furthermore, as suspected, the latter ¹³C NMR spectrum revealed this iPMP fraction to be more stereoregular than that

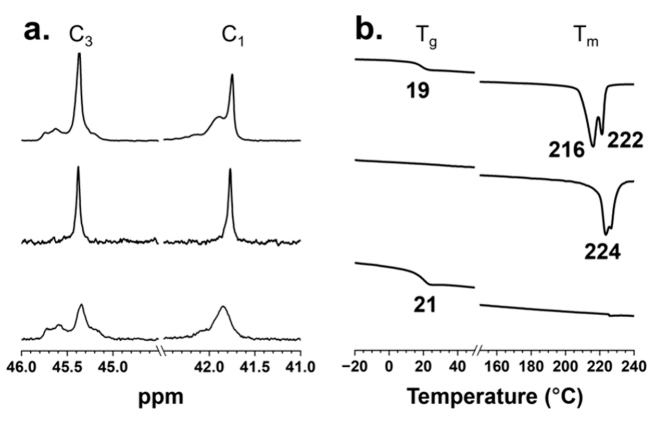


Figure 4. (a) Partial $^{13}\text{C}\{^1\text{H}\}$ (200 MHz, TCE- d_2 , 110 °C) NMR spectra showing ^{13}C resonances for C_1 and C_3 of PMP and (b) partial DSC traces [second heating ramp (10 °C/min)], with bold numbers indicating measured $T_{\rm g}$ and $T_{\rm m}$ values obtained according to (top) run 5, (middle) the insoluble fraction, and (bottom) the soluble fraction obtained by Soxhlet extraction with hexanes.

of the benchmark sample Ia of run 10 (cf Figures 3 and 4a), a result that we were initially at odds to explain. However, this simple fractionation could not be used to exclude the possible existence of a third stereoblock PMP fraction that could potentially be functioning as a blend compatibilizer between aPMP and iPMP. Accordingly, to better interrogate the tacticity composition of the PMP samples from runs 1–9, we next turned to crystallization elution fractionation (CEF) and high-temperature size exclusion chromatography (HT-SEC).

Figure 5 presents HT-SEC and CEF data for run 5, together with those of the insoluble and soluble fractions obtained from

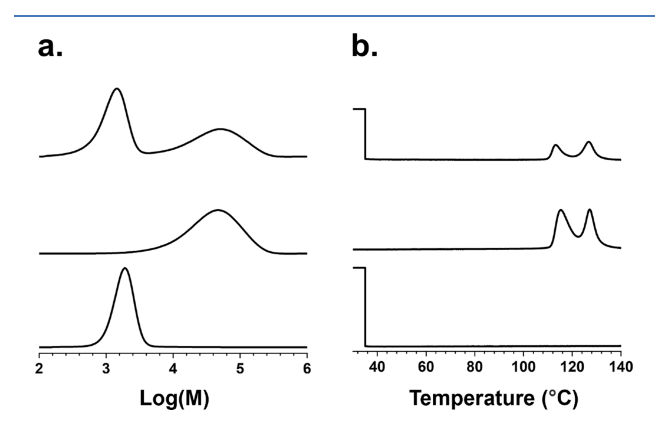


Figure 5. (a) HT-SEC and (b) CEF obtained according to (top) run 5, (middle) the insoluble fraction, and (bottom) the soluble fraction obtained by Soxhlet extraction with hexanes.

Soxhlet fractionation. Importantly, both sets of SEC traces clearly reveal the presence of only two components in the originally isolated PMP material, one of which is a lower molar mass amorphous fraction that elutes very early at low temperature and the second is a higher molar mass crystalline fraction that elutes at higher temperatures according to the CEF and HT-SEC analyses. Here, it is interesting to note the occurrence of two eluting crystalline fractions, which we have shown to also occur for the iPMP sample from run 10, as well as a commercial iPMP sample. We attribute these two fractions as arising from kinetic deposition during the CEF method of

two different dominant crystalline polymorphs of iPMP, of which five with differing solubilities have been previously identified by X-ray analyses and reported in the literature. In other words, no evidence could be found for the coexistence of a stereoblock fraction that might be serving as a blend compatibilizer between the aPMP and iPMP components. Finally, Figure 6 confirms that these HT-SEC and CEF results

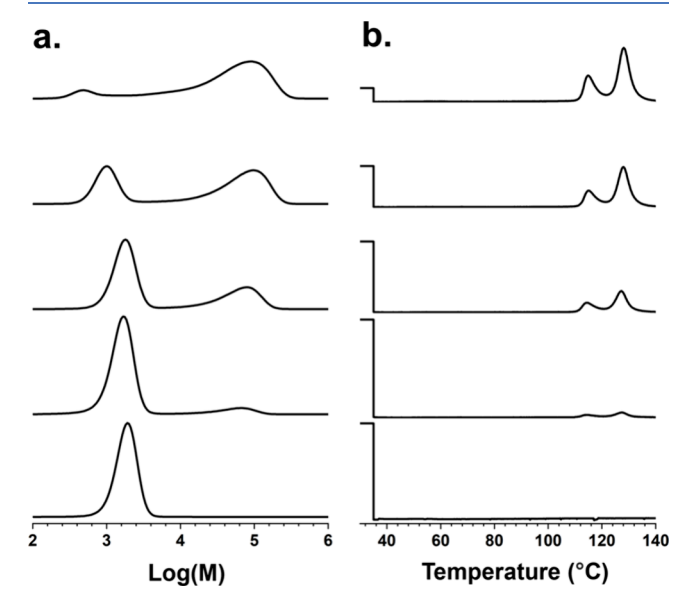


Figure 6. (a) HT-SEC and (b) CEF traces, obtained for runs 0, 2, 4, 6, and 8 of Table 1 (bottom to top).

and conclusions are consistent for all the PMP materials of Table 1. Succinctly, for mixtures of 1 and 2, a stereoblend of aPMP and iPMP is formed, rather than a stereoblock PMP product, and with the iPMP fraction increasing as the preinitiator ratio increasingly favors 2.

To summarize the present collection of results, we set out to investigate the strategy of producing new viscoelastic grades of PMP in controlled fashion by pitting two LCCTP processes against each other according to Scheme 1. The same symmetries and steric environments about the transition metals that enforce different stereochemical outcomes for propagation by active species obtained from 1 and 2 (i.e., atactic and isotactic, respectively) also dictate the relative rates of reversible chain exchange that occur between "like" (Hf/Hf or Zr/Zr) or "unlike" (Hf/Zr) propagators. In this case, it is clear that the less sterically encumbered aspecific Hf-based active species outcompete the isospecific Zr-based active species with respect to both a higher rate of chain growth propagation and domination for chain exchange with the fixed population of Zn-based surrogate centers. As a consequence, this leads to a lower molar mass fraction of aPMP by the former and higher stereoregularity of the iPMP fraction due to much less chain exchange occurring between enantiomeric forms of the latter. However, the most surprising and major finding of this work is the previously unreported ability of aPMP to serve as a property modifier for iPMP through the formation of blends. Although it remains to be confirmed through additional extended investigations, we propose that aPMP is compatible with the amorphous regions of iPMP, which then places constraints on the crystalline domain size (see Scheme 2). Finally, as a test of these hypotheses, a purposefully made blend (II) of separately prepared aPMP and

iPMP materials that conform to the fractions identified for run 3 (1:2 = 70:30) was obtained through solvent mixing and removal of volatiles. Gratifyingly, as Figure 1 reveals, a stressstrain characterization of II via DMA revealed very similar viscoelastic properties to those of between runs 2 and 3. Clearly, development of aPMP as a plasticizer for iPMP is far more desirable for recycling purposes than requiring formation of blends of iPMP with a structurally and chemically different class of property modifier. Further investigations are now in progress to explore the bulk structure and rheology of these new stereoblends of PMP and of their potential for new technological applications. In addition, given the wealth of structural diversity for CPAM group 4 metal complexes that we have previously shown to be competent as preinitiators for LCP and LCCTP, 8,9 we are further investigating the strategy of Scheme 1 to produce stereoblock polyolefins under optimized conditions through directed manipulation of the CPAM ligand steric environments about each active species. The results of these studies will be reported in due course.

ASSOCIATED CONTENT

5 Supporting Information

The Supporting Information is available free of charge at https://pubs.acs.org/doi/10.1021/acscatal.3c05570.

Experimental details; synthetic procedures; NMR data; SEC and CEF data; and DSC data (PDF)

AUTHOR INFORMATION

Corresponding Author

Lawrence R. Sita – Department of Chemistry and Biochemistry, University of Maryland, College Park, Maryland 20742, United States; orcid.org/0000-0002-9880-1126; Email: lsita@umd.edu

Authors

Danyon M. Fischbach – Department of Chemistry and Biochemistry, University of Maryland, College Park, Maryland 20742, United States

Charlotte M. Wentz – Department of Chemistry and Biochemistry, University of Maryland, College Park, Maryland 20742, United States

Saeid Mehdiabadi — Department of Chemical and Materials Engineering, University of Alberta, Edmonton, Alberta T6G 1H9, Canada

João Soares — Department of Chemical and Materials Engineering, University of Alberta, Edmonton, Alberta T6G 1H9, Canada; orcid.org/0000-0001-8017-143X

Complete contact information is available at: https://pubs.acs.org/10.1021/acscatal.3c05570

Notes

The authors declare the following competing financial interest(s): The corresponding author has a financial interest in the university spin-out company, Precision Polyolefins, LLC (PPL). This work did not involve any PPL personnel, funding, or other re-sources and all new intellectual property has been disclosed in accordance with state and federal requirements. *D.M.F. and C.M.W. are designated first co-authors.

ACKNOWLEDGMENTS

Support for this work was provided by a grant from the National Science Foundation (NSF) (CHE-2247554) to L.R.S for which he is grateful.

REFERENCES

- (1) (a) Vasile, C. (ed.) Handbook of Polyolefins. Marcel Dekker, Inc.: New York, 2000. (b) Kaminsky, W. (ed) Polyolefins: 50 years after Ziegler and Natta I: Polyethylene and Polypropylene. Advances in Polymer Science Vol. 257; Springer-Verlag: Heidelberg, 2013. (c) Kaminsky, W. (ed) Polyolefins: 50 years after Ziegler and Natta II: Polyolefins by Metallocenes and Other Single-Site Catalysts. Advances in Polymer Science Vol. 258. Springer-Verlag: Heidelberg, 2013. (d) Stürzel, M.; Mihan, S.; Mülhaupt, R. From Multisite Polymerization Catalysis to Sustainable Materials and All-Polyolefin Composites. Chem. Rev. 2016, 116, 1398–1433. (e) Al-AliAlMa'adeed, M.; Krupa, I. (eds) Polyolefin Compounds and Materials. Springer: Heidelberg, 2016.
- (2) (a) Arriola, D. J.; Carnahan, E. M.; Hustad, P. D.; Kuhlman, R. L.; Wenzel, T. T. Catalytic Production of Olefin Block Copolymers via Chain Shuttling Polymerization. Science 2006, 312, 714-719. (b) Sita, L. R. Ex uno plures ("out of one, many"): new paradigms for expanding the range of polyolefins through reversible group transfers. Angew. Chem., Int. Ed. 2009, 48, 2464-2472. (c) Hustad, P. D. Frontiers in Olefin Polymerization: Reinventing the World's Most Common Synthetic Polymers. Science 2009, 325, 704-707. (d) Kida, T.; Tanaka, R.; Hiejima, Y.; Nitta, K.; Shiono, T. Improving the strength of polyethylene solids by simple controlling of the molecular weight distribution. Polymer 2021, 218, No. 123526. (e) Tran, T. V.; Doi, L. H. Tunable modalities in polyolefin synthesis via coordination insertion catalysis. Eur. Polym. J. 2021, 142, No. 110100. (f) Zanchin, G.; Leone, G. Polyolefin thermoplastic elastomers from polymerization catalysis: advantages, pitfalls and future challenges. Prog. Polym. Sci. 2021, 113, No. 101342.
- (3) (a) Jubinville, D.; Esmizadeh, E.; Saikrishnan, S.; Tzoganakis, C.; Mekonnen, T. A comprehensive review of global production and recycling methods of polyolefin (PO) based products and their post-recycling applications. *Sustain. Mater. Technol.* **2020**, 25, No. e00188. (b) Geyer, R.; Jambeck, J. R.; Law, K. L. Production, Use, and Fate of All Plastics Ever Made. *Sci. Adv.* **2017**, 3, 19–24.
- (4) Ferreira-Filipe, D. A.; Paco, A.; Duarte, A. C.; Rocha-Santos, T.; Patrício Silva, A. L. Are Biobased Plastics Green Alternatives?- A Critical Review. *Int. J. Environ. Res. Public Health* **2021**, *18*, 7729.
- (5) Kots, P. A.; Vance, B. C.; Vlachos, D. G. Polyolefin plastic waste hydroconversion to fuels, lubricants, and waxes: a comparative study. *React. Chem. Eng.* **2021**, *7*, 41–45.
- (6) (a) Forni, L.; Invernizzi, R. Kinetics and mechanism of propylene to 4-methyl-1-pentene catalytic dimerization. *Ind. Eng. Chem. Process Des. Develop.* **1973**, *12*, 455–459. (b) Jin, H.; Jiang, H.; Yang, S.; He, G.; Guo, X. The catalytic characteristic and synthesis technique for 4-methyl-1-pentene over a potassium-supported superbase catalyst. *Chem. Eng. Commun.* **2019**, *206*, 346–354.
- (7) Lopez, L. C.; Wilkes, G. L.; Stricklen, P. M.; White, S. A. Synthesis, Structure, and Properties of Poly(4-methyl-1-pentene). *J. Macromol. Sci. Part C* **1992**, 32, 301–406.
- (8) For previous reports of two-state LCP, see: (a) Zhang, Y.; Keaton, R. J.; Sita, L. R. Degenerative transfer living Ziegler-Natta polymerization: application to the synthesis of monomodal stereoblock polyolefins of narrow polydispersity and tunable block length. J. Am. Chem. Soc. 2003, 125, 9062–9069. (b) Zhang, Y.; Sita, L. R. Stereospecific living Ziegler-Natta polymerization via rapid and reversible chloride degenerative transfer between active and dormant sites. J. Am. Chem. Soc. 2004, 126, 7776–7777. (c) Harney, M. B.; Zhang, Y.; Sita, L. R. Discrete, multiblock isotactic-atactic stereoblock polypropene microstructures of differing block architectures through programmable stereomodulated living Ziegler-Natta polymerization. Angew. Chem., Int. Ed. 2006, 45, 2400–2404. (d) Harney, M. B.; Zhang, Y.; Sita, L. R. Bimolecular control over polypropene

stereochemical microstructure in a well-defined two-state system and a new fundamental form: stereogradient polypropene. *Angew. Chem., Int. Ed.* **2006**, *45*, 6140–6144. (e) Giller, C.; Gururajan, G.; Wei, J.; Zhang, W.; Hwang, W.; Chase, D. Bruce; Rabolt, J. F.; Sita, L. R. Synthesis, Characterization, and Electrospinning of Architecturally Discrete Isotactic-Atactic Triblock Stereoblock Polypropene Elastomers. *Macromolecules* **2011**, *44*, 471–482. (f) Crawford, K. E.; Sita, L. R. Stereoengineering of poly(1,3-methylenecyclohexane) via two-state living coordination polymerization of 1,6-heptadiene. *J. Am. Chem. Soc.* **2013**, *135*, 8778–8781. (g) Crawford, K. E.; Sita, L. R. Regio- and stereospecific cyclopolymerization of bis(2-propenyl)-diorganosilanes and the two-state stereoengineering of 3,5-cis, isotactic poly(3,5-methylene-1-silacyclohexane)s. *ACS Macro Lett.* **2014**, *3*, 506–509.

(9) For previous reports of LCCTP and multistate LCCTP, see: (a) Zhang, W.; Sita, L. R. Highly efficient, living coordinative chaintransfer polymerization of propene with ZnEt2: practical production of ultrahigh to very low molecular weight amorphous atactic polypropenes of extremely narrow polydispersity. J. Am. Chem. Soc. 2008, 130, 442-443. (b) Zhang, W.; Wei, J.; Sita, L. R. Living coordinative Chain Transfer Polymerization and Copolymerization of Ethene, α -Olefins, and α , ω -Nonconjugated Dienes using Dialkylzinc as 'Surrogate' Chain-Growth Sites. Macromolecules 2008, 41, 7829-7833. (c) Wei, J.; Zhang, W.; Sita, L. R. Aufbaureaktion Redux: Scalable Production of Precision Hydrocarbons from AlR₃ (R = Et or iBu) by Dialkyl Zinc Mediated Ternary Living coordinative Chain Transfer Polymerization. Angew. Chem., Int. Ed. 2010, 49, 1768-1772. (d) Wei, J.; Zhang, W.; Wickham, R.; Sita, L. R. Programmable Modulation of Co-monomer Relative Reactivities for the Living Coordination Polymerization through Reversible Chain Transfer between 'Tight' and 'Loose' Ion Pairs. Angew. Chem.Int. Ed. 2010, 49, 9140-9144. (e) Wei, J.; Hwang, W.; Zhang, W.; Sita, L. R. Dinuclear Bis-Propagators for the Stereoselective Living coordinative Chain Transfer Polymerization of Propene. J. Am. Chem. Soc. 2013, 135, 2132-2135. (f) Wei, J.; Duman, L. M.; Redman, D. W.; Yonke, B. L.; Zavalij, P. Y.; Sita, L. R. N-Substituted Iminocaprolactams as Versatile and Low Cost Ligands in Main Group Metal Initiators for the Living Coordinative Chain Transfer Polymerization of α -Olefins. Organometallics 2017, 36, 4202-4207. (g) Wallace, M. A.; Zavalij, P. Y.; Sita, L. R. Enantioselective Living Coordinative Chain Transfer Polymerization: Production of Optically Active End-Group Functionalized (+)- or (-)-Poly(methylene-1,3-cyclopentane) via a Homochiral C₁-Symmetric Caproamidinate Hafnium Initiator. ACS Catal. 2020, 10, 8496-8502. (h) Wallace, M. A.; Wentz, C. M.; Sita, L. R. Optical Purity as a Programmable Variable for Controlling Polyolefin Tacticity in Living coordinative Chain Transfer Polymerization: Application to the Stereomodulated LCCTP of $\alpha_{,\omega}$ -Nonconjugated Dienes. ACS Catal. 2021, 11, 4583-4592. (i) Wallace, M. A.; Sita, L. R. Multi-State Living Degenerative and Chain Transfer Coordinative Polymerization of α -Olefins via Substoichiometric Activation. ACS Catal. 2021, 11, 9754-9760. (j) Wallace, M. A.; Sita, L. R. Temporal Control over Two- and Three-State Living Coordinative Chain Transfer Polymerization for Modulating the Molecular Weight Distribution Profile of Polyolefins. Angew. Chem., Int. Ed. 2021, 60, 19671-19678. (k) Wallace, M. A.; Burkey, A. A.; Sita, L. R. Phenyl-Terminated Polyolefins via Living Coordinative Chain Transfer Polymerization with ZnPh2 as a Chain Transfer Agent. ACS Catal. 2021, 11, 10170-10178. (1) Burkey, A. A.; Fischbach, D. M.; Wentz, C. M.; Beers, K. L.; Sita, L. R. Highly Versatile Strategy for the Production of Telechelic Polyolefins. ACS Macro Lett. 2022, 11, 402-409. (m) Burgenson, W. R.; Wentz, C. M.; Sita, L. R. Tailoring Glass Transition Temperature in as Series of Poly(methylene-1,3-cyclopentane-stat-cyclohexane) Statistical Copolymers. ACS Macro Lett. 2023, 12, 101-106. (n) Fischbach, D. M.; Krstic, K. A.; Sita, L. R. Versatile Production of Multivariate, Hyperdimensional End Group and Main Chain Functionalized Polyolefins. Angew. Chem., Int. Ed. 2023, 62, No. e202304725.

(10) Wentz, C. M.; Fischbach, D. M.; Sita, L. R. Stereomodulation of Poly(4-methyl-1-pentene): Adoption of a Neglected and Misunder-

stood Commercial Polyolefin. Angew. Chem., Int. Ed. 2022, 61, No. e202211992.

- (11) Müller, A. H. E.; Zhuang, R.; Yan, D.; Litvinenko, G. Kinetic Analysis of "Living" Polymerization Processes Exhibiting Slow Equilibria. 1. Degenerative Transfer (Direct Activity Exchange between Active and "Dormant" Species). Application to Group Transfer Polymerization. *Macromolecules* 1995, 28, 4326–4333.
- (12) For some leading references of sbPP obtained by non-living coordinative polymerization, see; (a) Baugh, L. S.; Canich, J. M. (eds.) Stereoselective Polymerization with Single-Site Catalysts. CRC Press: Boca Raton, 2008, and references cited therein. (b) Natta, G. Properties of isotactic, atactic, and stereoblock homopolymers, random and block copolymers of α -olefins. J. Polym. Sci. 1959, 34, 531–549. (c) Coates, G. W.; Waymouth, R. M. Oscillating Stereocontrol: A Strategy for the Synthesis of Thermoplastic Elastomeric Polypropylene. Science 1995, 267, 217–219.
- (13) (a) Lohse, D. J.; Wissler, G. E. Compatibility, and morphology of blends of isotactic and atactic polypropylene. J. Mater. Sci. 1991, 26, 743–748. (b) Sakurai, K.; MacKnight, W. J.; Lohse, D. J.; Schulz, D. N.; Sissano, J. A. Blends of amorphous-crystalline block copolymers with amorphous homopolymers. 2. Synthesis and characterization of Poly(ethylene-propylene) Diblock Copolymer and Crystallization Kinetics for the Blend with Atactic Polypropylene. Macromolecules 1994, 27, 4951–4951. (c) Nam, B.-K.; Park, O. O.; Kim, S.-C. Properties of isotactic polypropylene/atactic polypropylene blends. Macromol. Res. 2015, 23, 809–813. (d) Zhang, Z.; Zhang, R.; Huang, Y.; Lei, J.; Chen, Y.-H.; Tang, J.; Li, Z.-M. Efficient utilization of atactic polypropylene in its isotactic polypropylene blends via "structuring" processing. Ind. Eng. Chem. Res. 2014, 53, 10144–1-154. (14) Experimental details are provided in the Supporting Information.
- (15) Tacticity of a poly(α -olefin) can be defined by the relative percent of each possible sequence of adjacent stereocenters for a given number of repeat units, where m=meso and r=racemic relationships. At the pentad level of analysis, there are 10 possible configuration, with mmmm and rrrr representing the limiting isotactic and syndiotactic forms.
- (16) Alfano, F.; Boone, H. W.; Busico, V.; Cipullo, R.; Stevens, J. C. Polypropylene "Chain-Shuttling" at Enantiomorphous and Enantiopure Catalytic Species: Direct and Quantitative Evidence from Polymer Microstructure. *Macromolecules* **2007**, *40*, 7736–7738.
- (17) See for instance: (a) Lieber, S.; Brintzinger, H.-H. Propene Polymerization with Catalyst Mixtures Containing Different Ansa-Zirconocenes: Chain Transfer to Alkylaluminum Cocatalysts and Formation of Stereoblock Polymers. *Macromolecules* **2000**, 33, 9192–9199. (b) Tynys, A.; Eilertesen, J. L.; Seppa, J. V.; Rytter, E. Propylene polymerizations with a binary metallocene system chain shuttling caused by trimethylaluminum between active catalyst centers. *J. Polym. Sci., Part A* **2007**, 45, 1364–1376. (c) Descour, C.; Macko, T.; Cavallo, D.; Parkinson, M.; Hubner, G.; Villani, M.; Duchateau, R. Synthesis and characterization of iPP-sPP stereoblock produced by a binary metallocene system. *J. Polym. Sci. A Polym. Chem.* **2014**, 1422–1434. (d) Cannavacciuolo, F. D.; Vittoria, A.; Ehm, C.; Cipullo, R.; Busico, V. Polyolefin chain shuttling at ansa-metallocene catalysts: legend and reality. *Eur. Polym. J.* **2021**, 150, No. 110396.
- (18) (a) Kusanagi, H.; Takase, M.; Chatani, Y.; Tadokoro, H. Crystal structure of isotactic poly(4-methyl-1-pentene). *J. Polym. Sci. Polym. Phys. Ed.* **1978**, *16*, 131–142. (b) De Rosa, C. Crystal Structure of Form II of Isotactic Poly(4-methyl-1-pentene). *Macromolecules* **2003**, *36*, 6087–6094. (c) De Rosa, C.; Auriemma, F.; Borriello, A.; Corradini, P. Up-down disorder in the crystal structure of form III of isotactic poly(4-methyl-1-pentene). *Polymer* **1995**, *36*, 4723–4727. (d) Charlet, G.; Delmas, G.; Revol, J. F.; St John Manley, R. Effect of solvent on the polymorphism of poly(4-methyl-1-pentene). 1. Solution-grown single crystals. *Polymer* **1984**, 25, 1613–1618. (e) Charlet, G.; Delmas, G. Modification "V" of poly(4-methyl-1-pentene) from cyclopentane solutions and gels. *Polym. Bull.* **1982**, *6*, 367–373. (f) De Rosa, C.; Capitani, D.; Cosco, S. Solid-state ¹³C nuclear magnetic resonance spectra of four crystalline forms of

ACS Catalysis pubs.acs.org/acscatalysis Research Article

isotactic poly(4-methyl-1-pentene). Macromolecules 1997, 30, 8322-